Chemistry of Metals and Alloys

Chem. Met. Alloys 10 (2017) 30-39
Ivan Franko National University of Lviv
www.chemetal-journal.org

Crystal structures of the ternary compounds $Yb(Ga,Si)_{2-x}$

Taras DELENKO[1], Marina BOYKO[1], Natalia MUTS[1], Yaroslav TOKAYCHUK[1]*, Roman GLADYSHEVSKII[1]

[1] *Department of Inorganic Chemistry, Ivan Franko National University of Lviv, Kyryla i Mefodiya St. 6, 79005 Lviv, Ukraine*
* *Corresponding author. Tel.: +380-32-2394506; e-mail: tokaychuk@mail.lviv.ua*

Received May 19, 2017; accepted June 27, 2017; available on-line April 1, 2018

The existence of two ternary compounds with AlB_2- and α-$ThSi_2$-type structures was confirmed in the system Yb–Ga–Si at 600 and 500°C and their crystal structures were refined by the Rietveld method for different compositions. In addition, a new ternary phase was found at 500°C: $YbGa_{0.60(7)}Si_{1.27(7)}$ (structure type $GdSi_{1.4}$, Pearson symbol *oI*12, space group *Imma*, *a* = 4.0646(5), *b* = 4.0634(4), *c* = 14.0796(9) Å). The structure types AlB_2, α-$ThSi_2$, and $GdSi_{1.4}$ are members of the family of structures with trigonal-prismatic coordination of the smaller atoms. Substitution of Si atoms for Ga atoms in the ternary phases leads to increased dimensionality of the network formed by the *p*-element atoms.

Ytterbium / Gallium / Silicon / X-ray powder diffraction / Crystal structure

Introduction

Isothermal sections of the phase diagrams of the ternary systems *R*–Ga–Si have been constructed for *R* = Y (at 800°C) [1], La (600°C) [2], Ce (600°C) [3], Pr (600°C) [4], Nd (600°C) [5], Sm (600°C) [6], Gd (800°C) [7], and Er (600°C, 33.3-100 at.% Er) [8]. These systems are characterized by the formation of ternary phases along the line 33.3 at.% *R*, which adopt the binary structure types AlB_2 (Pearson symbol *hP*3, space group *P*6/*mmm*) [9] or α-$ThSi_2$ (*tI*12, $I4_1/amd$) [10]. The AlB_2-type phases represent solid solutions based on the binary digallides RGa_2, whereas the α-$ThSi_2$-type phases are ternary compounds with variable homogeneity ranges. Isotypic phases have also been reported for some other *R*–Ga–Si systems [11,12]. In the systems with *R* = Y, Nd, Sm, Er, and Tm, phases crystallizing with the structure type $GdSi_{1.4}$ (*oI*12, *Imma*), or the related type $Y(Ga_{0.4}Ge_{0.6})_{1.7}$ (*oI*16, *Imma*), have been reported at stoichiometric $R(Ga,Si)_2$ or off-stoichiometric $R(Ga,Si)_{2-x}$ compositions. Series of α-$ThSi_2$- and $Y(Ga_{0.4}Ge_{0.6})_{1.7}$-type ternary compounds in the systems *R*–Ga–Si were obtained by Ga self-flux synthesis and structurally characterized by X-ray single-crystal and powder diffraction in [13].

For the ternary system Yb–Ga–Si, alloys with an Yb-content of 33.3 at.% were investigated with the aim to find new phases with AlB_2-type or related structures, which might be the basis of new superconductor materials. The interest in these compounds was effectively motivated by the discovery of superconductivity in the compound MgB_2 (structure type AlB_2) with a critical temperature of 39 K, which is the highest among intermetallics [14]. Two ternary compounds, AlB_2-type $YbGa_{1.1}Si_{0.9}$ [15] and α-$ThSi_2$-type $YbGa_{0.76}Si_{1.24}$ [13], were reported. The homogeneity range at 800°C, thermal expansion, and superconducting properties of the AlB_2-type compound $YbGa_{1.49\text{-}1.12}Si_{0.51\text{-}0.88}$ were studied in [16,17]; the homogeneity range at 800°C and the electronic structure of $YbGa_{1.3\text{-}1.0}Si_{0.7\text{-}1.0}$ in [18]. It was shown that the ternary compound $YbGa_{1.1}Si_{0.9}$ is a type-II superconductor with T_c = 2.4 K [15], which decreases with increasing Ga content (T_c < 1.8 K for $YbGa_{1.41}Si_{0.59}$) [16]. Crystallographic data of ternary phases $R(Ga,Si)_2$ and $R(Ga,Si)_{2-x}$ formed in *R*–Ga–Si systems are summarized in Table 1.

The aim of the present work was to analyze the ternary system Yb–Ga–Si along the line 33.3 at.% Yb, investigate the crystal structures and homogeneity ranges of the ternary phases, and the phase equilibria at 500 and 600°C, based on X-ray powder diffraction. The crystal structure of the binary digallide $YbGa_2$, which delimits the $YbGa_{2-x}Si_x$ section, belongs to the structure type $CaIn_2$ (*hP*6, $P6_3/mmc$, *a* = 4.456, *c* = 7.187 Å) [29]. For the binary ytterbium disilicide two structure types, AlB_2 and α-$ThSi_2$, have been reported [30,31], and different off-stoichiometric compositions and structure types have been assigned: Yb_4Si_7 (Yb_4Si_7, *mP*22, $P2_1/m$) [32], $YbSi_{1.74}$ (AlB_2, *hP*3, *P*6/*mmm*) [33], Yb_3Si_5 (Th_3Pd_5, *hP*8, *P*-62*m*) [34], $Yb_2Si_{2.8}$ ($Ho_2Si_{2.67}$, *oS*24, *Cmcm*) [35], and $YbSi_{1.375}$ ($YbSi_{1.375}$, *oI*38, *Imm*2) [35].

Table 1 Crystallographic data for ternary phases with the structure types AlB_2 (*hP*3, *P*6/*mmm*), α-$ThSi_2$ (*tI*12, *I*4$_1$/*amd*), LaPtSi (*tI*12, *I*4$_1$*md*), $GdSi_{1.4}$ (*oI*12, *Imma*), $Y(Ga_{0.4}Ge_{0.6})_{1.7}$ (*oI*16, *Imma*), and $Lu_2Ga_{0.64}Si_{2.86}$ (*oS*28, *Cmcm*) in the systems *R*–Ga–Si.

Phase	Structure type	Unit-cell parameters, Å			Temperature	Ref.
		a	*b*	*c*		
$YGa_{2-1.64}Si_{0-0.36}$	AlB_2	…	…	…	800°C	[1]
$YGa_{1.5}Si_{0.5}$	α-$ThSi_2$	4.1012	–	14.290	800°C	[1]
$YGa_{1.26}Si_{0.74}$	α-$ThSi_2$	4.0935	–	14.255	as-cast	[13]
$YGa_{0.60-0.15}Si_{1.40-1.85}$	$GdSi_{1.4}$	4.068[a]	4.004[a]	13.62[a]	800°C	[1]
$Y_{1,11}Ga_{0,37}Si_{1,52}$	AlB_2	3.9214	–	4.123	800°C	[1]
$LaGa_{2-1.38}Si_{0-0.62}$	AlB_2	4.328-4.202	–	4.423-4.427	600°C	[2,6]
$LaGa_{1.18-0.50}Si_{0.82-1.50}$	α-$ThSi_2$	4.3162-4.2998	–	14.091-14.469	600°C	[2,6]
$LaGa_{0.84}Si_{1.16}$	α-$ThSi_2$	4.3087	–	14.285	as-cast	[13]
$LaGa_{0-1.0}Si_{2-1.0}$	α-$ThSi_2$	4.292-4.273	–	13.81-14.38	as-cast	[19]
$LaGa_{0-0.24}Si_{2-1.76}$	α-$ThSi_2$	4.2671-4.2973	–	13.924-14.002	600°C	[2,6]
$CeGa_{2-1.5}Si_{0-0.5}$	AlB_2	4.225-4.308	–	4.342-4.350	as-cast	[19]
$CeGa_{2-1.4}Si_{0-0.6}$	AlB_2	4.3102-4.2205	–	4.3205-4.3409	600°C	[3,6]
$CeGa_{1.4}Si_{0.6}$	AlB_2	4.188	–	4.336	as-cast	[20]
$CeGa_{1.30-0.65}Si_{0.70-1.35}$	α-$ThSi_2$	4.2510-4.2536	–	14.4949-14.1241	600°C	[3,6]
$CeGa_{1.3-0.5}Si_{0.7-1.5}$	LaPtSi[b]	4.236-4.325	–	14.06-14.09	as-cast	[19]
$CeGa_{0.87}Si_{1.13}$	α-$ThSi_2$	4.2426	–	14.274	as-cast	[13]
$CeGa_{0-0.2}Si_{2-1.8}$	α-$ThSi_2$	4.188-4.188	–	13.93-13.93	as-cast	[19]
$PrGa_{2-1.52}Si_{0-0.48}$	AlB_2	4.2816-4.1304	–	4.2896-4.3074	600°C	[4,6]
$PrGa_{1.30-0.67}Si_{0.70-1.32}$	α-$ThSi_2$	4.2184-4.2208	–	14.3757-14.0768	600°C	[4,6]
$PrGa_{1.02}Si_{0.98}$	α-$ThSi_2$	4.2189	–	14.296	as-cast	[13]
$PrGa_{0-0.42}Si_{2-1.58}$	α-$ThSi_2$	4.1788-4.1628	–	14.023-13.753	600°C	[4,6]
$NdGa_{2-1.55}Si_{0-0.45}$	AlB_2	4.2703-4.1971	–	4.2704-4.2882	600°C	[5,6]
$NdGa_{1.32-0.92}Si_{0.68-1.08}$	α-$ThSi_2$	4.20329-4.19192	–	14.4146-14.3002	600°C	[5,6]
$NdGa_{1.05}Si_{0.95}$	α-$ThSi_2$	4.1947	–	14.290	as-cast	[13]
$NdGa_{0.86-0.68}Si_{1.14-1.32}$	$GdSi_{1.4}$	4.21572-4.2073	4.19796-4.2040	14.1025-14.0781	600°C	[5,6]
$SmGa_{2-1.58}Si_{0-0.42}$	AlB_2	4.2378-4.1571	–	4.187-4.193	600°C	[6]
$SmGa_{1.4-1.0}Si_{0.6-1.0}$	α-$ThSi_2$	4.1641-4.1429	–	14.3859-14.2259	600°C	[6,21]
$SmGa_{1.01}Si_{0.99}$	α-$ThSi_2$	4.1405	–	14.209	as-cast	[13]
$SmGa_{0.95-0.65}Si_{1.05-1.35}$	$GdSi_{1.4}$	4.1777-4.1720	4.1464-4.1429	14.112-14.1003	600°C	[6]
$EuGa_{1.48-0.66}Si_{0.52-1.34}$	AlB_2	4.2431-4.1087	–	4.5829-4.5384	as-cast	[22]
EuGaSi	AlB_2	4.1687	–	4.5543	as-cast	[23]
$GdGa_{2-1.43}Si_{0-0.57}$	AlB_2	…	…	…	800°C	[7]
$GdGa_{2-1.43}Si_{0-0.57}$	AlB_2	4.224[c]	–	4.122[c]	600°C	[24]
$GdGa_{1.4-1.1}Si_{0.6-0.9}$	α-$ThSi_2$	4.127[d]	–	14.295[d]	800°C	[7]
$GdGa_{1.4-1.1}Si_{0.6-0.9}$	α-$ThSi_2$	4.088[e]	–	14.184[e]	600°C	[24]
$GdGa_{1.23}Si_{0.77}$	α-$ThSi_2$	4.1298	–	14.304	as-cast	[13]
$TbGa_{1.18}Si_{0.82}$	α-$ThSi_2$	4.090	–	14.222	as-cast	[13]
$DyGa_{1.40-1.22}Si_{0.60-0.78}$	α-$ThSi_2$	4.09349-4.08203	–	14.3106-14.2271	600°C	[25]
$DyGa_{1.24}Si_{0.76}$	α-$ThSi_2$	4.0811	–	14.2307	as-cast	[13]
$HoGa_{1.12}Si_{0.88}$	α-$ThSi_2$	4.0658	–	14.247	as-cast	[13]
$HoGa_{0.34}Si_{1.56}$	$Y(Ga_{0.4}Ge_{0.6})_{1.7}$[f]	3.970	4.020	13.401	as-cast	[13]
$ErGa_{1.48}Si_{0.52}$	α-$ThSi_2$	4.0547	–	14.310	600°C	[26]
$ErGa_{0.58-0.41}Si_{1.11-1.21}$	$GdSi_{1.4}$	3.9544-3.9646	4.0185-4.0385	13.3897-13.467	600°C	[26]
$ErGa_{0.41}Si_{1.43}$	$Y(Ga_{0.4}Ge_{0.6})_{1.7}$[f]	3.9653	4.0213	13.424	as-cast	[13]
$TmGa_{1.6}Si_{0.4}$	AlB_2	4.1548	–	3.9936	600°C	[27]
$TmGa_{0.32}Si_{1.50}$	$Y(Ga_{0.4}Ge_{0.6})_{1.7}$[f]	3.9283	3.9961	13.308	as-cast	[13]
$YbGa_{1.49-1.12}Si_{0.51-0.88}$	AlB_2	4.1272-4.1362	–	4.2129-4.2431	800°C	[16,17]
$YbGa_{1.3-1.0}Si_{0.7-1.0}$	AlB_2	4.126-4.151	–	4.237-4.253	800°C	[18]
$YbGa_{1.1}Si_{0.9}$	AlB_2	4.1275	–	4.2357	800°C	[15]
$YbGa_{0.76}Si_{1.24}$	α-$ThSi_2$	4.0957	–	14.220	as-cast	[13]
$Lu_2Ga_{0.64}Si_{2.86}$	$Lu_2Ga_{0.64}Si_{2.86}$[g]	3.9678	28.479	3.8138	as-cast	[13]

[a] composition not reported; [b] ternary variant of the structure type α-$ThSi_2$; [c] for $GdGa_{1.76}Si_{0.24}$; [d] for $GdGa_{1.12}Si_{0.88}$; [e] for $GdGa_{1.22}Si_{0.78}$; [f] derivative of the structure type $GdSi_{1.4}$ [28]; [g] derivative of the structure type $GdSi_{1.4}$.

Experimental

Alloys were synthesized from high-purity metals (Yb ≥ 99.85 mass%, Ga ≥ 99.99 mass%, Si ≥ 99.999 mass%) by arc melting, using a tungsten electrode and a water-cooled copper hearth under a Ti-gettered argon atmosphere. In order to compensate for uncontrolled Yb evaporation during the arc melting, 5 mass% excess of Yb was added to each sample. To achieve homogeneity, the samples were melted twice. After the synthesis the alloys were wrapped in tantalum foil, sealed in quartz ampoules under vacuum, and annealed at 600°C for 720 h, or at 500°C for 1680 h. Finally the ampoules with the samples were quenched into cold water.

Phase analysis and structure refinements were carried out using X-ray powder diffraction data collected at room temperature on a diffractometer DRON-2.0M (Fe *K*α-radiation) or STOE Stadi P (Cu $K\alpha_1$-radiation). The profile and structural parameters were refined by the Rietveld method, using the program package FullProf Suite [36]. Most of the samples were contaminated by small amounts of Yb_2O_3 (structure type $(Mn_{0.5}Fe_{0.5})_2O_3$, Pearson symbol *cI*80, space group *Ia*-3), which probably forms during partial decomposition of the samples under air.

Results

The interaction of the components along the line $YbGa_{2-x}Si_x$ at 600°C was deduced based on the phase analysis of 11 three-component alloys (Table 2) studied by X-ray diffraction. The Ga-rich samples contained the $CaIn_2$-type binary digallide as main phase, together with the binary compound $Yb_{0.89}Ga_{2.97}$ and an AlB_2-type ternary phase, indicating the existence of the corresponding three-phase equilibrium in the system Yb–Ga–Si at 600°C. The refined unit-cell parameters of the binary gallides agreed with those reported in the literature [29,37], indicating insignificant solubility of Si at 600°C.

Table 2 Crystallographic data for the phases in selected samples of the system Yb–Ga–Si at 600°C.

Alloy composition	Phases (content, mass%)	Structure type	Unit-cell parameters, Å		
			a	*b*	*c*
$Yb_{33.3}Ga_{61.7}Si_5$	$YbGa_2$ (70)	$CaIn_2$	4.4556(2)	–	7.1934(4)
	$YbGa_{1.1}Si_{0.9}$ (20)	AlB_2	4.1592(5)	–	4.2606(6)
	$Yb_{0.89}Ga_{2.97}$ (10)	$Yb_{0.89}Ga_{2.97}$	4.2041(4)	4.3336(10)	25.693(6)
$Yb_{33.3}Ga_{56.7}Si_{10}$	$YbGa_2$ (55)	$CaIn_2$	4.4543(3)	–	7.1957(4)
	$YbGa_{1.1}Si_{0.9}$ (40)	AlB_2	4.1591(4)	–	4.2611(5)
	$Yb_{0.89}Ga_{2.97}$ (5)	$Yb_{0.89}Ga_{2.97}$	4.2049(5)	4.3342(5)	25.697(3)
$Yb_{33.3}Ga_{51.7}Si_{15}$	$YbGa_{1.1}Si_{0.9}$ (73)	AlB_2	4.15888(11)	–	4.26103(18)
	$YbGa_2$ (25)	$CaIn_2$	4.4567(2)	–	7.1962(7)
	Yb_2O_3 (2)	$(Mn_{0.5}Fe_{0.5})_2O_3$	10.4396(9)	–	–
$Yb_{33.3}Ga_{46.7}Si_{20}$	$YbGa_{1.1}Si_{0.9}$ (86)	AlB_2	4.1588(2)	–	4.2603(3)
	$YbGa_2$ (12)	$CaIn_2$	4.4569(5)	–	7.1951(14)
	Yb_2O_3 (2)	$(Mn_{0.5}Fe_{0.5})_2O_3$	10.4343(9)	–	–
$Yb_{33.3}Ga_{37.7}Si_{29}$	$YbGa_{1.13}Si_{0.87}$ (99.4)	AlB_2	4.14640(5)	–	4.25080(6)
	Yb_2O_3 (0.6)	$(Mn_{0.5}Fe_{0.5})_2O_3$	10.4362(9)	–	–
$Yb_{33.3}Ga_{35.7}Si_{31}$	$YbGa_{1.08}Si_{0.92}$ (98.5)	AlB_2	4.13769(18)	–	4.24572(19)
	Yb_2O_3 (1.5)	$(Mn_{0.5}Fe_{0.5})_2O_3$	10.4355(12)	–	–
$Yb_{33.3}Ga_{33.3}Si_{33.3}$	$YbGa_{1.1}Si_{0.9}$ (80)	AlB_2	4.1338(2)	–	4.2439(3)
	$YbGa_{0.6}Si_{1.4}$ (17)	α-$ThSi_2$	4.1041(5)	–	14.176(3)
	Yb_2O_3 (3)	$(Mn_{0.5}Fe_{0.5})_2O_3$	10.4383(8)	–	–
$Yb_{33.3}Ga_{26.7}Si_{40}$	$YbGa_{0.6}Si_{1.4}$ (60)	α-$ThSi_2$	4.10450(14)	–	14.1770(8)
	$YbGa_{1.1}Si_{0.9}$ (38)	AlB_2	4.13308(18)	–	4.2438(3)
	Yb_2O_3 (2)	$(Mn_{0.5}Fe_{0.5})_2O_3$	10.4362(9)	–	–
$Yb_{33.3}Ga_{22.7}Si_{44}$	$YbGa_{0.64}Si_{1.36}$ (97.8)	α-$ThSi_2$	4.10310(6)	–	14.1766(2)
	Yb_2O_3 (2.2)	$(Mn_{0.5}Fe_{0.5})_2O_3$	10.4348(5)	–	–
$Yb_{33.3}Ga_{16.7}Si_{50}$	$YbGa_{0.6}Si_{1.4}$ (75)	α-$ThSi_2$	4.10136(14)	–	14.1709(6)
	Yb_3Si_5 (18)	Th_3Pd_5	6.5169(5)	–	4.0916(6)
	Si (5)	C	5.4276(8)	–	–
	Yb_2O_3 (2)	$(Mn_{0.5}Fe_{0.5})_2O_3$	10.432(3)	–	–
$Yb_{33.3}Ga_{10.7}Si_{56}$	$YbGa_{0.6}Si_{1.4}$ (50)	α-$ThSi_2$	4.09466(16)	–	14.0735(8)
	Yb_3Si_5 (43)	Th_3Pd_5	6.5175(3)	–	4.0925(3)
	Si (5)	C	5.4270(7)	–	–
	Yb_2O_3 (2)	$(Mn_{0.5}Fe_{0.5})_2O_3$	10.435(3)	–	–

The existence of ternary compounds with AlB_2- and α-$ThSi_2$-type structures was confirmed, and the two-phase region between them was located. The composition dependence of the unit-cell parameters corroborated the existence of homogeneity ranges for both compounds at 600°C. The Si-rich samples contained the ternary phase with α-$ThSi_2$-type structure, the binary compound Yb_3Si_5 (structure type Th_3Pd_5), and pure Si, displaying the corresponding three-phase equilibrium. Based on the similarity of the refined values of the unit-cell parameters of Yb_3Si_5 with those reported in the literature [34], the absence of any significant solubility of Ga can be assumed.

The crystal structures of the ternary compounds were refined from X-ray powder diffraction patterns of the samples $Yb_{33.3}Ga_{41.7}Si_{25}$, $Yb_{33.3}Ga_{32.7}Si_{34}$, and $Yb_{33.3}Ga_{26.7}Si_{40}$, collected on a STOE Stadi P diffractometer (Fig. 1). Experimental details and crystallographic data for the main phases in the samples are listed in Table 3. Atomic coordinates for the ternary phases $YbGa_{1.1}Si_{0.9}$ [15] and $YbGa_{0.76}Si_{1.24}$ [13] were chosen as starting models for the refinements of the structural parameters. The samples contained up to 2 mass% Yb_2O_3, for which only the scale factor and unit-cell parameter were refined. The background was defined by polynomial functions using the Fourier filtering technique. The final atomic coordinates, site occupancies and isotropic displacement parameters are listed in Table 4, and the interatomic distances, coordination numbers and polyhedra of the atoms can be found in Tables 5 and 6.

The phase analysis of the three-component $YbGa_{2-x}Si_x$ alloys annealed at 500°C confirmed the existence of the binary compounds $Yb_{0.89}Ga_{2.97}$, $YbGa_2$, YbGa, and Yb_3Si_5, as well as the ternary phases with AlB_2- and α-$ThSi_2$-type structures, and revealed the formation of a new ternary compound, $YbGa_{0.80(7)}Si_{1.07(7)}$, with $GdSi_{1.4}$-type structure. Crystallographic data for the individual phases in selected samples annealed at 500°C are listed in Table 7. The presence of phases with compositions different from $Yb(Ga,Si)_2$ can be explained by the excess of Yb added to the samples to compensate for loss during the synthesis.

As observed at 600°C, the above-mentioned binary compounds do not dissolve any significant amounts of the third component at 500°C. This was confirmed by the refined unit-cell parameters, which are in good agreement with those reported in the literature for the binary phases. The ternary compound with AlB_2-type structure has a larger unit cell at 500°C than at 600°C and is thus probably richer in Ga, which was confirmed by the structure refinement.

Table 3 Experimental details and crystallographic data for the main phases in the samples $Yb_{33.3}Ga_{41.7}Si_{25}$, $Yb_{33.3}Ga_{32.7}Si_{34}$, and $Yb_{33.3}Ga_{26.7}Si_{40}$ annealed at 600°C.

Sample, nominal composition		$Yb_{33.3}Ga_{37.7}Si_{29}$	$Yb_{33.3}Ga_{35.7}Si_{31}$	$Yb_{33.3}Ga_{22.7}Si_{44}$
Phase, refined composition		$YbGa_{1.13(1)}Si_{0.87(1)}$	$YbGa_{1.08(1)}Si_{0.92(1)}$	$YbGa_{0.64(1)}Si_{1.36(1)}$
Content, mass%		99.4(5)	98.5(6)	97.8(4)
Structure type		AlB_2	AlB_2	α-$ThSi_2$
Pearson symbol		*hP*3	*hP*3	*tI*12
Space group		*P*6/*mmm*	*P*6/*mmm*	$I4_1/amd$
Unit-cell parameters:	*a*, Å	4.14640(5)	4.13769(18)	4.10310(6)
	c, Å	4.25080(6)	4.24572(19)	14.1766(2)
Unit-cell volume *V*, Å^3		63.291(1)	62.950(5)	238.670(7)
Formula units per cell Z		1	1	4
Preferred orientation: value / [direction]		0.988(3) / [110]	0.992(4) / [110]	0.9882(16) / [110]
Diffractometer			STOE Stadi P	
Radiation type, wavelength λ, Å			Cu $K\alpha_1$, 1.54060	
Scanning mode			$\theta/2\theta$	
Range of 2θ, °			10.000-120.865	
Step size, °			0.015	
Profile parameters:	*U*	0.0142(17)	0.154(11)	0.0273(17)
	V	0.0134(18)	0.071(10)	0.0052(18)
	W	0.0084(4)	0.0038(18)	0.0090(4)
Shape parameter		0.652(5)	0.475(6)	0.563(5)
Asymmetry parameters		0.079(7), 0.0038(11)	0.076(8), 0.0297(15)	0.084(3), 0.0229(9)
Reliability factors:	R_B	0.0511	0.0800	0.0699
	R_F	0.0853	0.0747	0.0510
	R_p	0.0865	0.0860	0.0851
	R_{wp}	0.1190	0.1140	0.1130
	χ^2	2.61	7.43	4.63

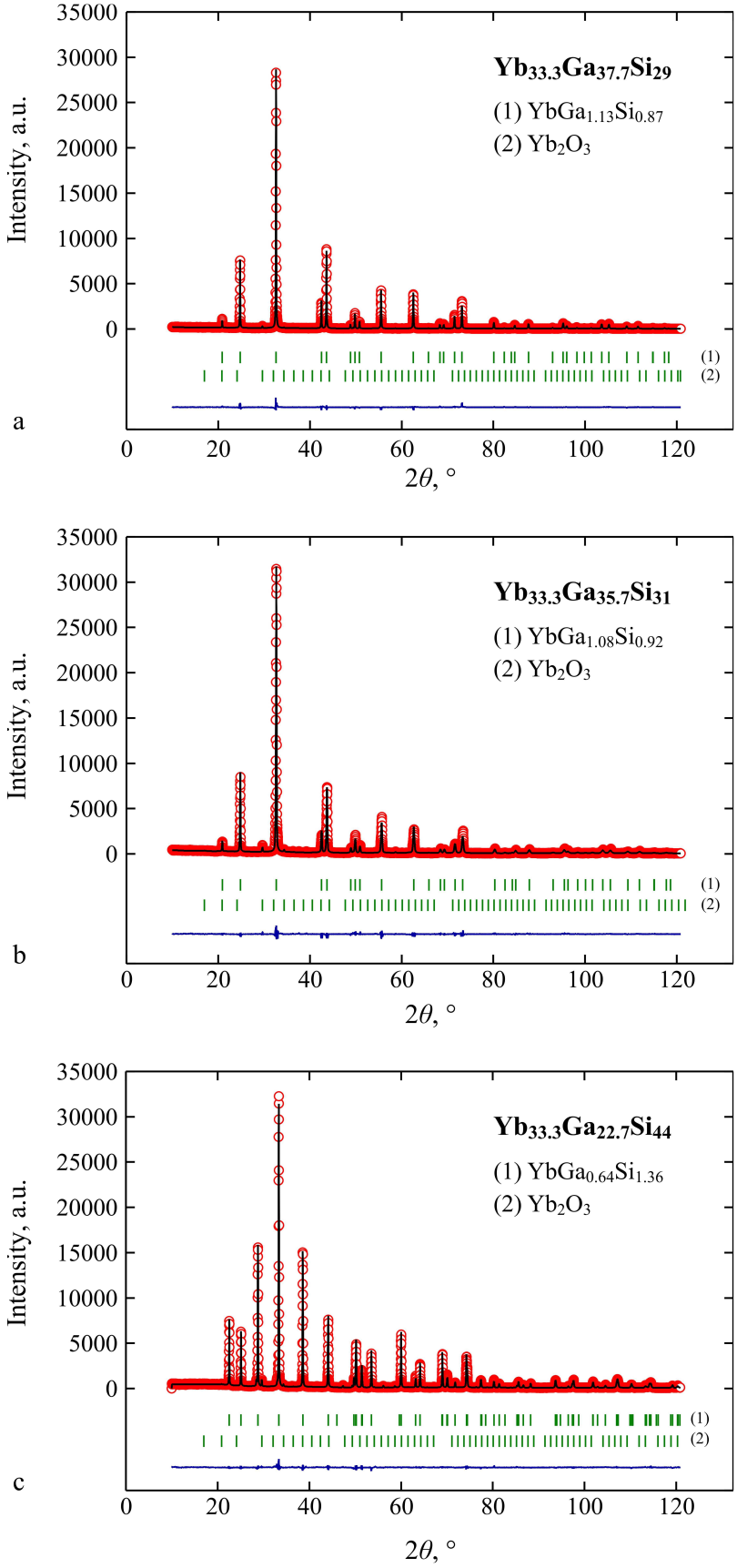

Fig. 1 Experimental (circles), calculated (continuous lines) and difference between experimental and calculated (bottom) X-ray powder diffraction patterns of the samples $Yb_{33.3}Ga_{37.7}Si_{29}$ (a), $Yb_{33.3}Ga_{35.7}Si_{31}$ (b), and $Yb_{33.3}Ga_{22.7}Si_{44}$ (c) annealed at 600°C. Vertical bars indicate the positions of the reflections of the different phases (Cu $K\alpha_1$ radiation).

Table 4 Atomic coordinates, site occupancies and isotropic displacement parameters for the ternary $Yb(Ga,Si)_2$ compounds in the system Yb–Ga–Si at 600°C.

Site	Wyckoff position	*x*	*y*	*z*	B_{iso}, Å^2
$YbGa_{1.13(1)}Si_{0.87(1)}$ (AlB_2, *hP*3, *P*6/*mmm*, *a* = 4.14640(5), *c* = 4.25080(6) Å)					
Yb	1*a*	0	0	0	0.86(2)
M (0.563(5)Ga+0.437(5)Si)	2*d*	⅓	⅔	½	1.24(4)
$YbGa_{1.08(1)}Si_{0.92(1)}$ (AlB_2, *hP*3, *P*6/*mmm*, *a* = 4.13769(18), *c* = 4.24572(19) Å)					
Yb	1*a*	0	0	0	0.72(3)
M (0.539(6)Ga+0.461(6)Si)	2*d*	⅓	⅔	½	1.37(7)
$YbGa_{0.64(1)}Si_{1.36(1)}$ (α-$ThSi_2$, *tI*12, *I*4$_1$/*amd*, *a* = 4.10310(6), *c* = 14.1766(2) Å)					
Yb	4*a*	0	¾	⅛	0.76(2)
M (0.322(4)Ga+0.678(4)Si)	8*e*	0	¼	0.29090(11)	1.61(5)

Table 5 Interatomic distances (δ), coordination numbers (CN) and coordination polyhedra in the structure of the AlB_2-type ternary compound in the system Yb–Ga–Si at 600°C.

Atoms	δ, Å		CN	Polyhedron
	$YbGa_{1.13(1)}Si_{0.87(1)}$	$YbGa_{1.08(1)}Si_{0.92(1)}$		
Yb – 12 *M*	3.20129(3)	3.1958(2)	20	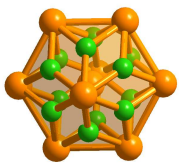
– 6 Yb	4.14640(4)	4.1377(2)		
– 2 Yb	4.25080(6)	4.2457(2)		$\underline{Yb}M_{12}Yb_8$
M – 3 *M*	2.39394(3)	2.3889(2)	9	
– 6 Yb	3.20129(3)	3.1958(2)		$\underline{M}Yb_6M_3$

Table 6 Interatomic distances (δ) coordination numbers (CN) and coordination polyhedra in the structure of the α-$ThSi_2$-type ternary compound $YbGa_{0.63(4)}Si_{1.37(4)}$ at 600°C.

Atoms	δ, Å	CN	Polyhedron
Yb – 8 *M*	3.1209(12)	20	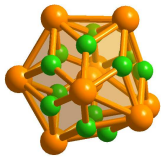
– 4 *M*	3.1367(6)		
– 4 Yb	4.09510(5)		
– 4 Yb	4.10310(6)		$\underline{Yb}M_{12}Yb_8$
M – 2 *M*	2.3566(11)	9	
– 1 *M*	2.385(2)		
– 3 Yb	4.09510(5)		
– 3 Yb	4.10310(6)		$\underline{M}Yb_6M_3$

It forms equilibria with the binary gallides $Yb_{0.89}Ga_{2.97}$, $YbGa_2$, and YbGa, and with the ternary α-$ThSi_2$-type phase. The latter is in equilibrium with Si, the binary silicide Yb_3Si_5, and the new ternary phase with $GdSi_{1.4}$-type structure. Both the ternary phase with α-$ThSi_2$- and that with $GdSi_{1.4}$-type structure have significant homogeneity ranges at 500°C, as indicated by the changes of the unit-cell parameters.

A Rietveld refinement was carried out on a powder diffraction pattern of the sample of nominal composition $Yb_{33.3}Ga_{26.7}Si_{40}$. The data were collected at room temperature on a diffractometer STOE Stadi P (Cu $K\alpha_1$-radiation) in the angular range

2θ = 20.000-72.610° with a step size of 0.015°. According to the preliminary phase analysis, the sample contained two phases with closely related structures (presumably both close to the structure type α-$ThSi_2$) and traces of Yb_2O_3. Deeper analysis of the powder pattern revealed splitting of some Bragg peaks of the main phase, indicating lowering of the symmetry from tetragonal to orthorhombic. The structure was successfully refined in the $GdSi_{1.4}$-type model, whereas the second phase was refined using the α-$ThSi_2$-type structure as model. The X-ray powder diffraction pattern of the sample $Yb_{33.3}Ga_{26.7}Si_{40}$ annealed at 500°C is shown in Fig. 2, and experimental details and crystallographic data for the individual phases in the sample are listed in Table 8. In total, 36 parameters were refined for three phases: sample shift, 3 scale factors, 6 cell parameters, 12 profile parameters (pseudo-Voigt profile function), 4 positional parameters, 5 displacement parameters, 4 occupancies and 2 texture parameters. The background was defined by a polynomial function using the Fourier filtering technique. The sample contained 0.4 mass% Yb_2O_3, for which only the scale factor and unit-cell parameter were refined. The atomic coordinates, site occupancies and isotropic displacement parameters are listed in Table 9, the interatomic distances, coordination numbers and polyhedra in Table 10.

Table 7 Crystallographic data for the phases in selected samples of the system Yb–Ga–Si at 500°C.

Alloy composition	Phases (content, mass%)	Structure type	Unit-cell parameters, Å		
			a	*b*	*c*
$Yb_{33.3}Ga_{50}Si_{16.7}$	$YbGa_{1.20}Si_{0.80}$ (73.1)	AlB_2	4.15632(10)	–	4.26753(14)
	$YbGa_2$ (20.9)	$CaIn_2$	4.4549(3)	–	7.1960(7)
	YbGa (6.0)	CuTi	3.4208(4)	–	3.9406(7)
$Yb_{33.3}Ga_{46.7}Si_{20.0}$	$YbGa_{1.2}Si_{0.8}$ (50)	AlB_2	4.1517(4)	–	4.2682(9)
	$YbGa_{0.85}Si_{1.15}$ (30)	α-$ThSi_2$	4.1269(5)	–	14.310(3)
	$Yb_{0.89}Ga_{2.97}$ (20)	$Yb_{0.89}Ga_{2.97}$	4.2051(6)	4.3321(6)	25.685(6)
$Yb_{33.3}Ga_{26.7}Si_{40}$	$YbGa_{0.80}Si_{1.07}$ (65.4)	$GdSi_{1.4}$	4.0646(5)	4.0634(4)	14.0796(9)
	$YbGa_{0.85}Si_{1.15}$ (34.2)	α-$ThSi_2$	4.1259(3)	–	14.3109(12)
	Yb_2O_3 (0.4)	$(Mn_{0.5}Fe_{0.5})_2O_3$	10.4389(13)	–	–
$Yb_{33.3}Ga_{16.7}Si_{50}$	$YbGa_{0.85}Si_{1.15}$ (50)	α-$ThSi_2$	4.1002(6)	–	14.170(2)
	$YbGa_{0.80}Si_{1.07}$ (30)	$GdSi_{1.4}$	4.053(2)	4.060(2)	14.068(8)
	Yb_3Si_5 (8)	Th_3Pd_5	6.5211(18)	–	4.0820(13)
	Yb_2O_3 (2)	$(Mn_{0.5}Fe_{0.5})_2O_3$	10.438(3)	–	–
$Yb_{33.3}Ga_5Si_{61.7}$	Yb_3Si_5 (60)	Th_3Pd_5	6.5189(3)	–	4.0878(2)
	$YbGa_{0.85}Si_{1.15}$ (30)	α-$ThSi_2$	4.0995(3)	–	14.085(2)
	Si (8)	C	5.4278(7)	–	–
	Yb_2O_3 (2)	$(Mn_{0.5}Fe_{0.5})_2O_3$	10.430(3)	–	–

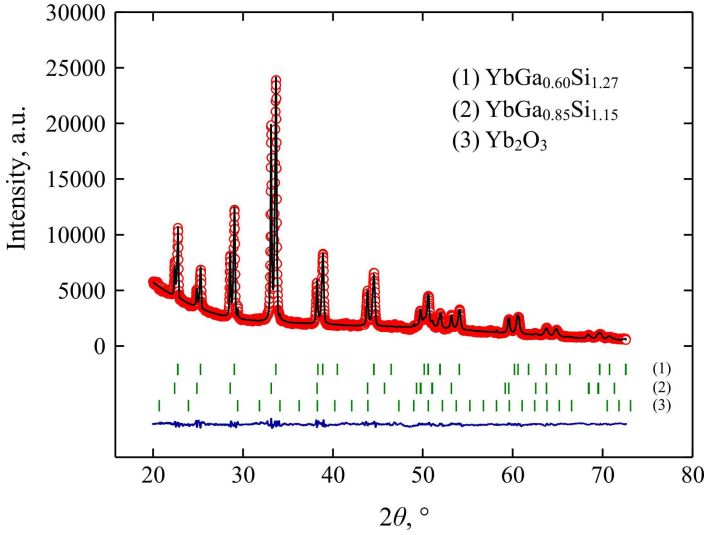

Fig. 2 Experimental (circles), calculated (continuous line) and difference between experimental and calculated (bottom) X-ray powder diffraction patterns of the sample $Yb_{33.3}Ga_{26.7}Si_{40}$ annealed at 500°C. Vertical bars indicate the positions of the reflections of the different phases (Cu $K\alpha_1$ radiation).

Table 8 Experimental details and crystallographic data for the phases in the sample $Yb_{33.3}Ga_{26.7}Si_{40}$ annealed at 500°C.

Phase		$YbGa_{0.60(7)}Si_{1.27(7)}$	$YbGa_{0.85(3)}Si_{1.15(3)}$	Yb_2O_3
Content, mass%		65.4(6)	34.2(4)	0.4(1)
Structure type		$GdSi_{1.4}$	α-$ThSi_2$	$(Mn_{0.5}Fe_{0.5})_2O_3$
Pearson symbol		*oI*12	*tI*12	*cI*80
Space group		*Imma*	$I4_1/amd$	*Ia*-3
Unit-cell parameters:	*a*, Å	4.0646(5)	4.1259(3)	10.4389(13)
	b, Å	4.0634(4)	–	–
	c, Å	14.0796(9)	14.3109(12)	–
Unit-cell volume *V*, Å^3		232.54(4)	243.62(3)	1137.5(3)
Formula units per cell Z		4	4	16
Preferred orientation: value / [direction]		0.867(4) / [110]	0.788(6) / [110]	–
Profile parameters:	*U*	0.90(6)	0.80(7)	0.90
	V	-0.28(4)	-0.34(5)	-0.28
	W	0.053(6)	0.055(8)	0.053
Shape parameter		0.529(16)	0.73(2)	0.529
Asymmetry parameters		0.114(12), 0.0547(16)	0.019(19), 0.001(2)	–
Reliability factors:	R_B	0.0342	0.0525	–
	R_F	0.0411	0.0524	–
	R_p		0.0379	
	R_{wp}		0.0516	
	χ^2		6.28	

Table 9 Atomic coordinates, site occupancies and isotropic displacement parameters for the ternary compounds $YbGa_{0.60(7)}Si_{1.27(7)}$ and $YbGa_{0.85(3)}Si_{1.15(3)}$ at 500°C.

Site	Wyckoff position	*x*	*y*	*z*	B_{iso}, Å^2
$YbGa_{0.60(7)}Si_{1.27(7)}$ ($GdSi_{1.4}$, *oI*12, *Imma*, *a* = 4.0646(5), *b* = 4.0634(4), *c*= 14.0796(9) Å)					
Yb	4*e*	0	¼	0.6314(11)	0.63(8)
*M*1 (0.48(5)Ga+0.52(5)Si)	4*e*	0	¼	0.0606(13)	1.35(15)
*M*2 (0.12(3)Ga+0.75(4)Si)	4*e*	0	¼	0.2295(16)	2.0(2)
$YbGa_{0.85(3)}Si_{1.15(3)}$ (α-$ThSi_2$, *tI*12, $I4_1/amd$, *a* = 4.1259(3), *c*= 14.3109(12) Å)					
Yb	4*a*	0	¾	⅛	0.72(2)
M (0.425(13)Ga+0.575(13)Si)	8*e*	0	¼	0.2921(4)	1.48(5)

Table 10 Interatomic distances (δ) and coordination numbers (CN) of the atoms in the structures of the ternary compounds $YbGa_{0.60(7)}Si_{1.27(7)}$ and $YbGa_{0.85(3)}Si_{1.15(3)}$ at 500°C.

$YbGa_{0.60(7)}Si_{1.27(7)}$			
Atoms		δ, Å	CN
Yb	– 2 *M*2	2.8722(19)	20
	– 4 *M*1	3.042(8)	
	– 4 *M*2	3.188(12)	
	– 2 *M*1	3.382(19)	
	– 2 Yb	3.909(19)	
	– 2 Yb	4.0634(4)	
	– 2 Yb	4.0646(5)	
	– 2 Yb	4.221(19)	
*M*1	– 2 *M*1	2.653(17)	9
	– 1 *M*2	2.38(3)	
	– 4 Yb	3.042(8)	
	– 2 Yb	3.382(19)	
*M*2	– 2 *M*2	2.113(9)	9
	– 1 *M*1	2.38(3)	
	– 2 Yb	2.882(19)	
	– 4 Yb	3.188(12)	

$YbGa_{0.85(3)}Si_{1.15(3)}$			
Atoms		δ, Å	CN
Yb	– 8 *M*	3.149(2)	20
	– 4 *M*	3.158(4)	
	– 4 Yb	4.1259(3)	
	– 4 Yb	4.1299(3)	
M	– 1 *M*	2.373(8)	9
	– 2 *M*	2.389(4)	
	– 3 Yb	3.149(2)	
	– 3 Yb	3.158(4)	

Discussion

On increasing the Si content along the line YbGa$_{2-x}$Si$_x$ the formation of YbM_2 intermetallic compounds with three closely related structures was observed: CaIn$_2$ (binary YbGa$_2$), AlB$_2$ (ternary phase) and α-ThSi$_2$ (ternary phase). These simple structure types are characterized by only two atom sites, one for the Yb atoms and one for the *p*-element atoms, which in the case of the ternary phases is occupied by a statistical mixture of Ga and Si atoms. The coordination polyhedra of the Yb atoms in the CaIn$_2$- and AlB$_2$-type structures are similar and can be described as 20-vertex pseudo Frank-Kasper polyhedra of composition YbM_{12}Yb$_8$, represented as hexagonal prisms M_{12} with all faces centered by Yb atoms. The polyhedron around the Yb atom in the α-ThSi$_2$-type phase also contains 20 atoms and can be described as an elongated *gyrobifastigium*, or gabled rhombohedron (a stereohedron with 4 rectangular and 4 pentagonal faces), formed by the smaller atoms, with all faces centered by Yb atoms. In all these structures the *p*-element atoms are coordinated by trigonal prisms of Yb atoms with three additional atoms situated above the rectangular faces. The orthorhombic structure type GdSi$_{1.4}$ is a deformation derivative of the tetragonal structure type α-ThSi$_2$, and the coordination polyhedra are similar. In the case of the GdSi$_{1.4}$-type ternary phase YbGa$_{0.60}$Si$_{1.27}$ the orthorhombic deformation is a consequence of the presence of vacancies on one of the sites occupied by Ga and Si atoms. The shortest interatomic distance in the structure (2.113(9) Å) is observed between positions of the partly occupied site *M*2 and the value indicates strong interaction between the atoms. In the closely related structure type Y(Ga$_{0.4}$Ge$_{0.6}$)$_{1.7}$ one of the sites with mixed Ga/Ge occupation is split and moved out of one of the mirror planes [28]. In our case refinement of such structural details was prevented by the quality of the X-ray powder diffraction pattern.

The structure types AlB$_2$, CaIn$_2$, α-ThSi$_2$, and GdSi$_{1.4}$ are members of the family of structures with trigonal-prismatic coordination of the smaller atoms according to the systematic of structure types proposed by Kripyakevich [38]. In all these structures the trigonal prisms formed by the larger atoms are interconnected *via* all their triangular and rectangular faces. In the α-ThSi$_2$-type structures the trigonal prisms in consecutive layers along the 4-fold axis (crystallographic direction [001]) are rotated by 90° with respect to each other. The pseudo-tetragonal structure type GdSi$_{1.4}$ is a deformed derivative of the α-ThSi$_2$ type and is built from trigonal prisms formed by the larger atoms surrounding the smaller atoms in the same manner. The structure of the Th$_3$Pd$_5$-type binary compound Yb$_3$Si$_5$, which is in equilibrium with the α-ThSi$_2$- and GdSi$_{1.4}$-type ternaries in the system Yb–Ga–Si, is an ordered vacancy derivative of the structure type AlB$_2$ and consequently also belongs to the family of structures with trigonal-prismatic coordination of the smaller atoms.

The structure types AlB$_2$ and α-ThSi$_2$ show different connections of the small atoms. In the AlB$_2$-type structures these atoms form flat graphite-like nets perpendicular to the 6-fold axis (crystallographic direction [001]), whereas in the α-ThSi$_2$-type structures they form a three-dimensional network (Fig. 3). The shortest interatomic distances in the structures of the ternary compounds are the distances between the *p*-element atoms, which form the above-mentioned networks.

Conclusions

Three ternary compounds Yb(Ga,Si)$_{2-x}$ with significant homogeneity ranges form in the system Yb–Ga–Si. Their structures belong to the structure types AlB$_2$, α-ThSi$_2$, and GdSi$_{1.4}$, which are members of the family of structures with trigonal-prismatic coordination of the smaller atoms. Substitution of Si atoms for Ga atoms increases the dimensionality of the network formed by the *p*-element atoms from flat graphite-like nets in the AlB$_2$-type phase to a three-dimensional network in the α-ThSi$_2$- and GdSi$_{1.4}$-type phases.

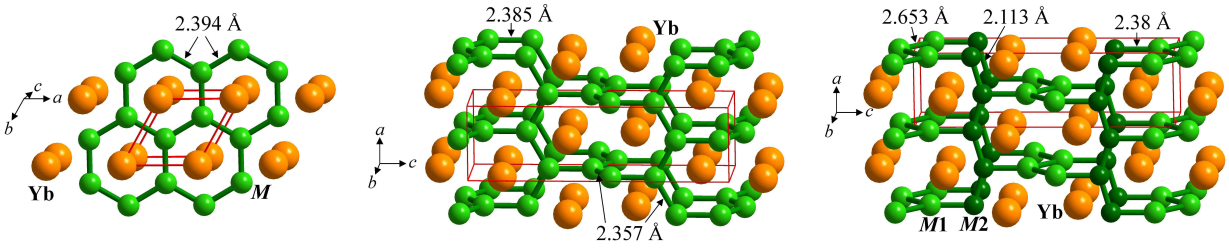

YbGa$_{1.13}$Si$_{0.87}$
(AlB$_2$, *hP*3, *P*6/*mmm*)

YbGa$_{0.63}$Si$_{1.37}$
(α-ThSi$_2$, *tI*12, *I*4$_1$/*amd*)

YbGa$_{0.60}$Si$_{1.27}$
(GdSi$_{1.4}$, *oI*12, *Imma*)

Fig. 3 Networks formed by the *p*-element atoms in the structures of the ternary compounds in the system Yb–Ga–Si.

Acknowledgements

This work was carried out under the grant of the Ministry of Education and Science of Ukraine No. 0115U003257.

References

[1] M.V. Speka, *PhD Thesis*, Kyiv, 2003 (in Ukrainian).
[2] Ya.O. Tokajchuk, A.A. Fedorchuk, I.R. Mokra, *Pol. J. Chem.* 74 (2000) 745-748.
[3] Ya. Tokaychuk, A. Fedorchuk, I. Mokra, O. Bodak, *Visn. Lviv. Univ., Ser. Khim.* 41 (2002) 40-45.
[4] Ya. Tokaychuk, A. Fedorchuk, I. Mokra, *Visn. Lviv. Univ., Ser. Khim.* 39 (2000) 25-29.
[5] Ya.O. Tokaychuk, A.O. Fedorchuk, O.I. Bodak, I.R. Mokra, *J. Alloys Compd.* 36 (2004) 764-69.
[6] Ya.O. Tokaychuk, *PhD Thesis*, Lviv, 2004 (in Ukrainian).
[7] N.V. Golovata, *PhD Thesis*, Kyiv, 1999 (in Ukrainian).
[8] S.Ya. Pukas *PhD Thesis*, Lviv, 2008 (in Ukrainian).
[9] W. Hoffmann, W. Jäniche, *Naturwissenschaften* 23 (1935) 851.
[10] G. Brauer, A. Mitius, *Z. Anorg. Allg. Chem.* 249 (1942) 325-339.
[11] P. Villars, K. Cenzual (Eds.), *Pearson's Crystal Data – Crystal Structure Database for Inorganic Compounds*, ASM International, Materials Park, OH, USA, Release 2016/17.
[12] P. Villars, K. Cenzual, R. Gladyshevskii (Eds.), *Handbook of Inorganic Substances 2016*, Walter de Gruyter, Berlin, 2016. 1877 p.
[13] G.M. Darone, B. Hmiel, J. Zhang, Sh. Saha, K. Kirshenbaum, R. Greene, J. Paglione, S. Bobev, *J. Solid State Chem.* 201 (2013) 191-203.
[14] J. Nagamatsu, N. Nakagawa, T. Muranaka, Y. Zenitani, J. Akimitsu, *Nature* 410 (2001) 63-64.
[15] M. Imai, A. Sato, T. Aoyagi, T. Kimura, Y. Matsushita, N. Tsujii, *J. Am. Chem. Soc.* 130 (2008) 2886-2887.
[16] N. Tsujii, Y. Ito, H. Yoshikawa, H. Kitazawa, M. Imai, H. Yamaoka, I. Jarrige, H. Oohashi, T. Tochio, K. Handa, J. Ide, H. Atsuta, *Chem. Mater.* 22 (2010) 4690-4699.
[17] N. Tsujii, M. Imai, H. Kitazawa, *J. Phys. Conf. Ser.* 344 (2012) 012012.
[18] C.P. Fang, C.S. Lue, Y.D. Hsu, Y.K. Kuo, *J. Appl. Phys.* 108 (2010) 073911.
[19] H. Mori, N. Sato, T. Satoh, *Solid State Commun.* 49 (1984) 955-958.
[20] K.R. Priolkar, S.M. Pattalwar, P.K. Mishra, P. Raj, A. Sathyamoorthy, S.K. Dhar, V.C. Sahni, P.R. Sarode, R.B. Prabhu, *Solid State Commun.* 104 (1997) 71-73.
[21] Ya.O. Tokaychuk, A.O. Fedorchuk, I.R. Mokra, *Visn. Lviv. Univ., Ser. Khim.* 38 (1999) 31-33.
[22] T.S. You, J.T. Zhao, R. Pöttgen, W. Schnelle, U. Burkhardt, Y. Grin, G.J. Miller, *J. Solid State Chem.* 182 (2009) 2430-2442.
[23] T.S. You, Y. Grin, G. J. Miller, *Inorg. Chem.* 46 (2007) 8801-8811.
[24] O. Mykhalichko, R. Gladyshevskii, *Visn. Lviv. Univ., Ser. Khim.* 53 (2012) 3-11.
[25] O.S. Holdak, Ya.O. Tokaychuk, A.O. Fedorchuk, I.R. Mokra, *Visn. Lviv. Univ., Ser. Khim.* 38 (1999) 31-33.
[26] S.Ya. Pukas, R. Cerny, M.B. Manyako, R.E. Gladyshevskii, *Ukr. Khim. Zh.* 73(11) (2007) 18-25.
[27] O.S. Holdak, I.R. Mokra, A.O. Fedorchuk, O.R. Myakush, Ya.O. Tokaychuk, *Coll. Abstr. VIII Int. Conf. Cryst. Chem. Intermet. Compd.*, Lviv, Ukraine (2002) 103.
[28] V.Y. Markiv, N.N. Belyavina, M.V. Speka, *J. Alloys Compd.* 285 (1999) 167-171.
[29] A. Iandelli, *Z. Anorg. Allg. Chem.* 330 (1964) 221-232.
[30] V.M. Koleshko, V.F. Belitsky, A.A. Khodin, *Thin Solid Films* 141 (1986) 277-285.
[31] S.C. Peter, M.G. Kanatzidis, *Z. Anorg. Allg. Chem.* 638 (2012) 287-293.
[32] S. Brutti, D. Nguyen Manh, D.G. Pettifor, *Intermetallics* 14 (2006) 1472-1486.
[33] A. Palenzona, P. Manfrinetti, S. Brutti, G. Balducci, *J. Alloys Compd.* 348 (2003) 100-104.
[34] A. Iandelli, A. Palenzona, G.L. Olcese, *J. Less-Common Met.* 64 (1979) 213-220.
[35] C.M. Kubata, F. Krumeich, M. Wörle, R. Nesper, *Z. Anorg. Allg. Chem.* 631 (2005) 546-555.
[36] J. Rodriguez-Carvajal, *Commission on Powder Diffraction (IUCr), Newsletter* 26 (2001) 12-19.
[37] M. Tillard, C.H.E. Belin, *Inorg Chem.* 48 (2009) 9250-9257.
[38] P.I. Kripyakevich, *Structure Types of Intermetallic Compounds*, Nauka, Moscow, 1977, 288 p. (in Russian).